Atmos. Chem. Phys. Discuss., 13, 23139–23171, 2013
www.atmos-chem-phys-discuss.net/13/23139/2013/
doi:10.5194/acpd-13-23139-2013

Atmospheric Chemistry and Physics Discussions

A sea spray aerosol flux parameterization encapsulating wave state

J. Ovadnevaite[1], A. Manders[2], G. de Leeuw[2,3,4], C. Monahan[1], D. Ceburnis[1], and C. D. O'Dowd[1]

[1]School of Physics and Centre for Climate and Air Pollution Studies, Ryan Institute, National University of Ireland Galway, University Road, Galway, Ireland
[2]TNO, Utrecht, the Netherlands
[3]Finnish Meteorological Institute (FMI), Climate Change Unit, Helsinki, Finland
[4]Department of Physics, University of Helsinki, Finland

Received: 11 July 2013 – Accepted: 12 August 2013 – Published: 3 September 2013

Correspondence to: J. Ovadnevaite (jurgita.ovadnevaite@nuigalway.ie)

Published by Copernicus Publications on behalf of the European Geosciences Union.

Abstract

A new sea spray source function (SSSF), termed Oceanflux Sea Spray Aerosol or OSSA, was derived based on in-situ sea spray measurements along with meteorological/physical parameters. Submicron sea spray fluxes derived from particle number concentration measurements at the Mace Head coastal station, on the west coast of Ireland, were used together with open-ocean eddy correlation flux measurements from the Eastern Atlantic (SEASAW cruise). In the overlapping size range, the data for Mace Head and SEASAW were found to be in a good agreement, which allowed deriving the new SSSF from the combined dataset spanning the dry diameter range from 15 nm to 6 µm. The sea spray production was parameterized in terms of 5 log-normal modes and the Reynolds number instead of the more commonly used wind speed, thereby encapsulating important influences of wave height and history, friction velocity and viscosity. This formulation accounts for the different flux relationships associated with rising and waning wind speeds since these are included in the Reynolds number. Furthermore, the Reynolds number incorporates the kinematic viscosity of water, thus the SSSF inherently includes a sea surface temperature dependence. The temperature dependence of the resulting SSSF is similar to that of other in-situ derived source functions and results in lower production fluxes for cold waters and enhanced fluxes from warm waters as compared with SSSF formulations that do not include temperature effects.

1 Introduction

Sea spray aerosol (SSA) is an important component of the aerosol population in the marine environment, and given that 70 % of the Earth's surface is covered by oceans, sea spray contributes significantly to the global aerosol budget (Vignati et al., 2010). In addition, sea spray plays an important role in climate, with both direct (Mulcahy et al., 2008) and indirect radiative effects (O'Dowd et al., 1999). Sea spray aerosol particles are formed at the sea surface mainly by breaking waves via bubble bursting

ACPD
13, 23139–23171, 2013

(Blanchard, 1963) and, at elevated wind speeds, by direct tearing of wave crests (Monahan et al., 1986). When a wave breaks, air is entrained into the water and dispersed into a cloud of bubbles (Thorpe, 1992), which rise to the surface and burst. The near-surface wind speed, commonly measured and expressed at a reference height of 10 m, U_{10}, is thought to be the dominant factor affecting sea-spray production. However, different formulations of the size-dependent sea spray source functions (SSSF) in terms of only U_{10} vary widely for the same U_{10} and rising or waning winds produce different production fluxes (Callaghan et al., 2008; Goddijn-Murphy et al., 2011; Norris et al., 2012; Ovadnevaite et al., 2012). Considerable effort has been devoted to linking SSA production to more fundamentally relevant physical parameters, such as wind stress on the surface, or whitecap fraction, with the expectation that such approaches might lead to better constraining the production flux than a formulation in terms of wind speed alone. However, at a given U_{10}, wind stress on the surface can vary by a factor of two (Drennan et al., 2005) and white cap fraction by a factor of 10 or more (Lewis and Schwartz, 2004; Anguelova and Webster, 2006); this variation is likely due to variability in the wave field, surface properties, and the like. Factors that are expected to affect the SSA production flux are those affecting sea state, such as fetch (the upwind distance over the water of nearly constant wind velocity) and atmospheric stability (often parameterized as the air-sea temperature difference), which also affects vertical transport; seawater temperature and salinity; and the presence, amount, and nature of surface-active substances. The production of sea-spray aerosol was recently reviewed by de Leeuw et al. (2011) who critically examined recent laboratory and field experimental results on sea-spray production, on the enrichment in organic matter, and on the measurement and parameterization of whitecap coverage, and placed it in the context of previous understanding which was comprehensively reviewed by Lewis and Schwartz (2004). The study indicated that there is still considerable uncertainty in the production of sea spray aerosol and suggested that existing submicron number flux parameterizations appear to over-predict boundary layer number concentrations compared to what is actually measured.

ACPD
13, 23139–23171, 2013

In this study we derive a new sea spray source function, termed Oceanflux Sea Spray Aerosol or OSSA, which covers the dry particle size range from 15 nm to a 6 µm in diameter and uses a direct fit of the size-dependent flux observations to a wave breaking parameter (Reynolds number). This approach includes the wind history and wave state along with the sea surface water temperature and salinity in one parameter.

2 Description of the data

The source function was derived from the combination of three data sets: Mace Head observations, SEASAW open-ocean eddy-covariance measurements and ECMWF-modelled wave parameters. Mace Head and SEASAW data did not cover the same time and region, but both datasets were representative for the North East Atlantic during low biological productivity.

2.1 Mace Head observations

Submicron aerosol particle size distributions were used, which were measured at the Mace Head Atmospheric Research Station on November 2010. Mace Head is located on the west coast of Ireland facing the North East Atlantic. Station details are described in O'Connor et al. (2008). All aerosol instruments are located in the shore laboratory at about 100 m from the coastline. They are connected to the laminar flow community air sampling system, which is constructed from a 100 mm diameter stainless-steel pipe with the main inlet at 10 m above ground level. The performance of this inlet is described in Kleefeld et al. (2002). Details on the Mace Head representativeness of marine aerosol can be found in the recent study by O'Dowd et al. (2013).

Aerosol size distributions and number concentrations were measured using a scanning mobility particle sizer (SMPS) system. The system comprised of a differential mobility analyzer (DMA, TSI model 3071), a condensation particle counter (TSI model

ACPD
13, 23139–23171, 2013

3010), and an aerosol neutralizer (TSI 3077). Before their sizes were measured, the particles were dried to a relative humidity below 40 %.

The wind speed and direction were measured on the 10 m tower by a Vector Instruments wind monitor (model W200P/A100 L).

The High Resolution Time of Flight Aerosol Mass Spectrometer (HR-ToF-AMS or AMS) (DeCarlo et al., 2006) was used for chemical composition measurements and was routinely calibrated according to the methods described by Jimenez et al. (2003) and Allan et al. (2003). The HR-ToF-AMS measurements were performed with a time resolution of 5 min and a vaporizer current of 1.12 A (corresponding to a vaporizer temperature of ~ 650 °C). The composition dependent collection efficiency (CE) (Middlebrook et al., 2012) was applied for the measurement periods discussed in this study. Sea salt concentrations were measured following the method described in Ovadnevaite et al. (2012).

Data obtained during the occurrence of an elevated- sea salt concentration plume over the North East Atlantic described in Ovadnevaite et al. (2012) were used to derive the submicron SSSF. The plume was detected as the wind direction backed northerly into the clean sector at Mace Head (between 190–300°) and the wind speed increased to a peak value of 26 $m\,s^{-1}$. Sea salt plumes measured by the AMS coincided with an increase in aerosol hygroscopicity from a typical sulphate hygroscopic growth factor (GF) of 1.6 to a GF of 2.2, which is characteristic of pure sea salt particles. As the measurements were undertaken during the low biological activity period, all other chemical compounds approached very low background "winter" concentrations (e.g. nss-sulphate mass < 10 $ng\,m^{-3}$; organic mass < 60 $ng\,m^{-3}$; black carbon mass < 10 $ng\,m^{-3}$; nitrate mass < 17 $ng\,m^{-3}$ and ammonium mass below the detection limit of 38 $ng\,m^{-3}$). A more detailed description of this sea spray aerosol event can be found in Ovadnevaite et al. (2012).

ACPD
13, 23139–23171, 2013

2.2 Open-ocean eddy correlation fluxes (SEASAW)

Since Mace Head data covers only the submicron part of the SSSF, fluxes of larger sea spray aerosol particles measured during the SEASAW campaign (described and analysed in detail in Norris et al., 2012) were used to complement the Mace Head derived SSSF. The SEASAW open-ocean flux data set consists of 111 valid measurements during a cruise in the eastern North Atlantic Ocean, 21 March–12 April 2007. Wind speed conditions ranged from 3 to 18 m s^{-1}, and the ship was actively relocated to areas with high wind speed conditions. The biological activity, estimated from satellite data and aerosol volatility measurements, was low. Data were obtained with the CLASP instrument (Hill et al., 2008), measuring aerosol particle concentrations in 16 size channels covering a range of 0.17–9.5 µm radius at ambient relative humidity. Sea spray aerosol fluxes were measured using the eddy covariance technique, with sampling records of 28 min. Flux estimates were corrected for the relative humidity flux, and results were harmonized to represent fluxes for particle radii at 80 % relative humidity. In the literature, it is common to use either the dry particle diameter (D_{dry}) or the radius at 80 % RH (R_{80}); in fact these two conventions come down to the same numerical value as for sea salt particles a wet radius at 80 % RH equals the dry diameter. More details can be found in study by Norris et al. (2012). When using these data to derive a SSSF there were some limitations that should be mentioned. Firstly, the scatter in the data was considerable (order of magnitude), which is inherent to the measurement technique. Secondly, a net flux was measured, which included both the production flux and the deposition. Norris et al. (2012) indicate that the difference between the production flux and the net flux is important for supermicron particles larger than about R_{80} = 5 µm, however, this difference becomes insignificant for particles smaller than 1 µm.

2.3 ECMWF modelled wave fields

Wave data from the ECMWF wave model (WAM) were used in this study to derive the Reynolds number from wave characteristics. Data were globally available on 6 hly

ACPD
13, 23139–23171, 2013

basis for a $0.5 \times 0.5^{\circ}$ longitude–latitude resolution. The ERA-interim reanalysis product was used to get a consistent data set over several years. We have used the wind velocity, mean drag coefficient, and significant height of wind waves. WAM assimilates wave height data derived from satellite altimetry data from JASON-1, JASON–2 and ENVISAT (Abdalla et al., 2010).

3 Approach

3.1 Breaking waves and Reynolds number

As indicated above, sea spray generation is directly related to wind-induced breaking of waves, which entrains air into the ocean surface layer. The entrained air breaks up into bubbles which rise to the surface where they break and produce film and jet droplets (Blanchard, 1986). The surface manifestation of a bubble plume is referred to as a whitecap and the fraction of whitecaps covering the ocean surface, i.e. whitecap fraction parameterized in terms of a forcing parameter, is often used as the basis for the formulation of a sea spray source function (Lewis and Schwartz, 2004). Based on consideration of the energy flux from wind to waves, Wu (1979) proposed that wave breaking, and therefore whitecap fraction, should be proportional to u_*^3 or $U_{10}^{3.75}$ where u_* is the friction velocity. At the same time, Monahan and Muircheartaigh (1980) proposed their $U_{10}^{3.41}$ power law derived from several whitecap observation data sets. However, the wave state depends not only on the actual wind speed but also on wind history (fetch, increasing or decreasing winds), leading to developing or well-developed waves, with different wave steepness. Based on physical considerations of wave breaking, Zhao and Toba (2001) proposed the use of a dimensionless breaking wave parameter, or alternatively a Reynolds number, Re_{H}, which includes the friction velocity, the height of wind waves and the viscosity of the air. They also proposed to replace the viscosity of air with the viscosity of water that is conceptually more relevant, and which was later reinforced by Woolf (2005). The resulting expression for the

ACPD
13, 23139–23171, 2013

Reynolds number Re_{H_w} is presented below:

$$Re_{H_w} = u_* H_s / \nu_w \quad (1)$$

Here H_s is the significant wave height and ν_w is the viscosity of water. The viscosity of sea water depends on temperature and salinity (Sharqawy et al., 2010), the effects of which are thus implicitly included in a sea spray source function formulated in terms of Re_{H_w}. Re_{H_w} increases with increasing temperature (decreasing viscosity) and vice versa. The use of either the breaking wave parameter or the Reynolds number brings results from several laboratory experiments and in-situ observations for whitecap coverage together (Zhao and Toba, 2001), unlike the use of parameters like (non-dimensional) fetch or wave age. The good correlation between whitecap coverage and breaking wave parameter was further demonstrated by Goddijn-Murphy et al. (2011). Also for the current data set the advantage of using Re_{H_w} instead of wind speed was obvious: the differences in wind speed dependence of the SSA fluxes for rising or waning winds (Ovadnevaite et al., 2012) disappeared when the fluxes were parameterized in terms of Re_{H_w} (an example is presented in Fig. S1, Supplement). Reduced scatter of data points improved R^2 from 0.95 to 0.98 and reduced the chi square from 16.4 to 5.8.

The Re_{H_w} expression used in this paper is obtained by replacing u_* in Eq. 1 with $u_* = C_d^{1/2} U_{10}$, because the drag coefficient, C_d, and U_{10} are readily available from WAM:

$$Re_{H_w} = C_d^{1/2} U_{10} H_s / \nu_w \quad (2)$$

In other words, the Reynolds number based on physical considerations (wave energy balance) incorporates both wind and wave parameters. In addition, it also includes temperature and salinity effects through the water viscosity.

ACPD
13, 23139–23171, 2013

3.2 Submicron flux calculations

Submicron aerosol particles are expected to be uniformly mixed in the marine boundary layer (Lewis and Schwartz, 2004), thus an effective SSA production flux, $F_{\mathrm{eff}}(D)$, was estimated from the SSA number concentration ($N(D)$) divided by a filling time (τ) and multiplied by the marine boundary layer height (H_{MBL}):

$$F_{\mathrm{eff}}(D) = \frac{N(D) \times H_{\mathrm{MBL}}}{\tau} \quad (3)$$

Here D is the dry particle diameter.

The atmospheric boundary layer height, derived from ground-based LIDAR measurements using the Temporal Height Tracking (THT) algorithm (Haeffelin et al., 2012; Milroy et al., 2012), was observed to vary between 720 and1290 m above ground level over the plume duration period. The filling time τ was assumed to be approximately 1.5–2 days, as discussed in Ovadnevaite et al. (2012) who used a similar method to derive the submicron sea spray aerosol mas flux.

The local wind speed at Mace Head was representative of the open ocean situation further upwind, obtained from NOAA Air Resources Laboratory, as illustrated in Fig. 1a. Moreover, Fig. 1c–d indicates the good agreement between wind speeds measured at Mace Head and the wind speeds modelled by ECMWF for the area upwind to Mace Head (Fig. 1b) which, together with ECMWF model data for significant wave heights and drag coefficients, was used to calculate Re_{H_w}. Since ECMWF data were provided with a resolution of only 6 h, too coarse for application to the relatively short event studied here, they were interpolated to a resolution of 10 min. Modelled, interpolated and measured data are presented in Fig. 1c and d.

Although the background mass concentration (as measured at $\sim 4\,\mathrm{m\,s^{-1}}$ wind speed) was insignificant (Ovadnevaite et al., 2012), the background number size distribution was subtracted from the number distributions at higher wind speeds.

The dry deposition was assumed to be negligible for the submicron particles (Hoppel et al., 2002), because the deposition flux contributes only 2–4 % to the total flux. During

ACPD
13, 23139–23171, 2013

the period of Mace Head observations used here, there were practically no clouds or precipitation and therefore the contribution of wet-deposition and coalescence removal processes to the total flux were negligible.

3.3 Error propagation

The SSSF uncertainty was evaluated by applying error propagation rules (Taylor, 1997). The submicron aerosol flux was calculated from the number size distribution (N), the boundary layer height (H) and the filling time (τ) (see Eq. 3), therefore, the resulting uncertainty was equal to $\sqrt{\Delta N^2 + \Delta H^2 + \Delta \tau^2}$. The SMSP measurement uncertainty $\Delta N \sim 10$–$20\,\%$ (Wiedensohler et al., 2012), $\Delta H \sim 15$–$20\,\%$ (Milroy et al., 2012) and $\Delta \tau \sim 50\,\%$ (Ovadnevaite et al., 2012), therefore, the resulting submicron SSSF uncertainty is in the range of 55–60 %.

Since the derived Reynolds number was used instead of direct U_{10} measurements, the uncertainty due to Re_{H_w} calculations (see Eq. 2) was evaluated accordingly: $\sqrt{\Delta {C_d}^2 + \Delta {U_{10}}^2 + \Delta {H_s}^2}$; the uncertainty in ΔH_s is ~ 2–$5\,\%$, $\Delta U_{10} \sim 10\,\%$, $\Delta C_d \sim 15\,\%$, which resulted in an overall Re_{H_w} uncertainty of $\sim 20\,\%$.

4 Results

The size dependent SSA production flux ($\mathrm{d}F(D)/\mathrm{dlog}D$) was derived from $\mathrm{d}N(D)/\mathrm{dlog}D$ data (measured by SMPS) by calculating $F(D)$ from $N(D)$ using Eq. (3). Submicron data then were combined with the measured supermicron $\mathrm{d}F(D)/\mathrm{dlog}D$ data and averaged over $1\,\mathrm{m\,s^{-1}}$ wind speed bins. An average Reynolds number was also calculated for each of these bins. Combined $\mathrm{d}F/\mathrm{dlog}D$ data points are presented in Fig. 2 for different wind speeds. In the overlapping size range (at $\sim 300\,\mathrm{nm}$) the two data sets show very good agreement, except for the measurements at lowest and the highest wind speeds, although these were still within the uncertainty limits described above. For every wind speed bin, five lognormal size distributions were fitted to the result-

ACPD
13, 23139–23171, 2013

ing dF/dlog$D$ distribution (Fig. 3). This resulted in a five-modal SSA flux formulation in terms of the Reynolds number Re_{H_w} with different coefficients for each mode:

$$\frac{\mathrm{d}F}{\mathrm{dlog}D} = \sum_{i=1}^{5} \frac{F_i(Re_{H_w})}{\sqrt{2\pi}D\ln\sigma_i} \exp\left(-\frac{1}{2}\left(\frac{\ln\left(\frac{D}{\mathrm{CMD}_i}\right)}{\ln\sigma_i}\right)^2\right) \quad (4)$$

Here dF/dlog$D$ is the size dependent SSA production flux, i – mode number, $F_i(Re_{H_w})$ – the flux for mode i, D – dry particle diameter, σ – geometrical standard deviation, CMD – count median diameter. All parameters used in Eq. (4) are listed in Table 1, including the SSA production flux relationship with Re_{H_w} through the $F_i(Re_{H_w})$. Below, this source function is referred to as the OSSA source function.

The forcing parameter was included into $F_i(Re_{H_w})$, because other variables (CMD and σ) did not depend on the wind speed or Reynolds number (Re_{H_w}). The dependence of F_i on Re_{H_w} is shown in Fig. 3b together with the measurement data. The Re_{H_w} dependence is distinctly different for each mode, which suggests different physical processes for the production of particles of different sizes, as was earlier suggested by Monahan's pioneering studies (Monahan et al., 1986). The study by Monahan et al. also indicated a different wind speed for the onset of the production by the different mechanisms. Therefore, different intercepts for submicron and supermicron aerosol particles (Re_{H_w} at $1e^5$ and $2e^5$ respectively in Table 1) were not unexpected. The Re_{H_w} threshold is a factor of 10 higher than the value of 10^4 proposed by Zhao and Toba (2001), but it is consistent with results from the study by Callaghan et al. (2008), which suggested a wind speed threshold for the onset of white-capping of $\sim 3.7\,\mathrm{m\,s^{-1}}$, corresponding to $Re_{H_w} \sim 1e^5$ at given wave height and sea surface temperature (SST) conditions.

Measured and parameterized fluxes for two different values of Re_{H_w} are presented in Fig. 4, which shows d$F(D)$/dlog$D$ vs. D together with the calculated uncertainties. Figure 4 shows that the parameterized fluxes represent the observations well within

ACPD
13, 23139–23171, 2013

the uncertainty range which suggests that the main driving processes were captured correctly.

4.1 SSSF intercomparison

A comparison of the OSSA sea spray source function and other commonly used or recently (last decade) developed source functions at 8 m s^{-1} wind speed (de Leeuw et al., 2011) is presented in Fig. 5. This wind speed was selected as the most common one in the real ambient environment. Since the OSSA-SSSF depends on the Reynolds number instead of the wind speed directly, Re_{H_w} was calculated using Eq. (2) for a wind speed of 8 m s^{-1} and other parameters relevant to the conditions for which this source function was derived ($C_d = 2.15e^{-3}$, $H_s = 1.23$, $\nu_w = 1.34e^{-6}$).

The OSSA-SSSF is on the lower side as compared to other parameterizations. As noted by de Leeuw et al. (2011) and Ovadnevaite et al. (2012), source functions based on Monahan's whitecap parameterization tend to result in higher atmospheric submicron number/mass concentrations than those typically measured. A recent EMEP unified model intercomparison study (Tsyro et al., 2011) shows that model calculations using the Mårtensson et al. (2003) and Gong (2003) SSSF overestimate atmospheric concentrations of Na by 8 % to 46 % in comparison with EMEP observations. The higher overestimation was observed for the winter season, which is consistent with the results presented in Ovadnevaite et al. (2012): the stronger flux- wind speed relationship of Mårtensson et al. (2003) or Gong (2003) would result in higher overestimation of sea salt mass concentrations during the high wind speed periods which are more manifest in the winter season.

The OSSA-SSSF has been evaluated by comparing the resulting sea spray mass with independent AMS measurements at Mace Head, which were not used in the derivation of the OSSA-SSSF. However, the data can only be used to validate the submicron part of the spectrum. In order to achieve this, the OSSA number flux was simulated for a particle size range directly comparable to the AMS measurement size

ACPD
13, 23139–23171, 2013

range (D_p = 0.03–0.58 µm or vacuum aerodynamic diameter, as measured in the HR-ToF-AMS, D_{va} = 0.05–1 µm), converted to a corresponding mass flux and integrated over the size range. This was done for a range of wind speeds and the results are shown in Fig. 6, together with AMS-derived mass fluxes (Ovadnevaite et al., 2012) and the respective uncertainties. The production flux derived using the OSSA-SSSF is within the uncertainty ranges of the AMS mass fluxes although it overestimated the mass concentration from 0 % (at 5 m s^{-1} wind speed) to 80 % (at 20 m s^{-1} wind speed). However, the agreement between the OSSA-SSSF and the AMS-derived SSA mass fluxes is significantly better than that between AMS and other SSSFs presented in Ovadnevaite et al. (2012). The largest discrepancy between the SSA mass fluxes obtained with the OSSA-SSSF and measured with the AMS was caused by the large uncertainty in supermicron aerosol distributions (see SEASAW description in Sect. 2) since SSA particles in this size range have the highest contribution to the SSA mass. As shown in Fig. 3, particles in mode 5 contribute significantly to the submicron aerosol number concentration (see F_5 in Fig. 3a) and therefore also to the resulting mass flux together with the inherent uncertainties.

In addition, the variation in the HR-ToF-AMS aerodynamic lens cut-off could have had an effect on the mass concentrations measured by the HR-ToF-AMS. The typical HR-ToF-AMS aerodynamic lens cut-off of 1 µm (50 % transmission efficiency for the particle vacuum aerodynamic diameter, D_{va}, of 1 µm or mobility diameter, D_m, of 0.58 µm) was applied to the number flux derived from this study in order to compare different methods. However, the best agreement between the masses derived from the OSSA-SSSF and measured by the AMS was achieved when an upper cut-off of 0.9 µm is selected.

4.2 An estimate of the global production flux

The annual mean production flux was calculated for the year 2006 using a simple modelling tool that uses the global meteorology and the wave characteristics from ECMWF to calculate the emission fluxes. Meteorological fields and wave characteristics are pre-

ACPD
13, 23139–23171, 2013

sented in the Supplement (Fig. S2). Mass and number fluxes were calculated for particles with dry diameters < 1 µm. 3 hly sea surface temperature and U_{10} from ECMWF IFS analysis, 6 hly C_d, significant height of wind waves from WAM ERA-Interim and sea surface temperature (SST) dependent viscosity, assuming a constant salinity of 35, were used to calculate Re_{H_w} using Eq. (2). The Reynolds number was then used in the parameterization (4) with the parameters of Table 1. As expected, Fig. 7 shows higher production fluxes for the regions with stronger winds. In addition, water temperature effects, incorporated in Re_{H_w} through the viscosity, enhance the production in the warm waters on both sides of the equator, and reduced it for the colder water regions with respect to an exercise in which the OSSA source function was used with constant viscosity (not shown). In addition, the wave state contributes to Re_{H_w} modulating the impact of wind speed alone and thus bringing an extra dimension to the interpretation.

Global instantaneous fluxes derived from the meteorological and wave data are presented in Fig. 8, which shows a comparison of these fluxes with those derived with the same modelling tool but using the Gong (2003) and Jaeglé et al. (2011) source functions. These two source functions are similar with the difference that Jaeglé et al. incorporate temperature effects based on a comparison between model computations and MODIS observations of the aerosol optical depth (AOD). The comparisons were made for instantaneous global data (2 January 2006, 00:00 UTC) for number fluxes of particles with a dry diameter smaller than 0.15 or 1 µm and for the mass flux of particles smaller than 1 µm. Fluxes computed using the Gong SSSF are presented on both left and right panels in black dots, while the fluxes computed using the OSSA-SSSF are presented in coloured circles on the left panel and those using the Jaeglé SSSF in coloured circles on the right panel. The differences in the fluxes due to the SST effect, as compared to the Gong SSSF, are obvious for both the OSSA and the Jaeglé et al. SSSF. Higher fluxes are produced at higher temperatures (red colours in the Fig. 8), while at lower temperature regimes (blue colours) the fluxes are lower. In addition to the spread due to SST, the OSSA-SSSF also accounts for wave state, which reduces the effect of temperature on the fluxes and brings some of the low tem-

ACPD
13, 23139–23171, 2013

perature points closer to the Gong-derived fluxes. This is due to the on average larger values of the wave height and drag coefficient in the lower temperature regions (Fig. S2, Supplement). As an example, the low flux values calculated using the Jaeglé SSSF at high wind speeds and at low SST (Fig. 8a, right panel) are not observed in the fluxes calculated with the OSSA-SSSF (Fig. 8a, left panel) which are all higher due to the effects of waves. The submicron number flux resulting from our function is quite evenly distributed around Gong's function for all wind speeds (Fig. 8a, left panel). However, the number fluxes for the Aitken mode particles, important for cloud formation, are lower than those obtained using Gong, especially at higher wind speeds (Fig. 8b, left panel). In addition, the OSSA SSSF derived submicron mass fluxes are considerably lower than those derived using Gong's SSSF, at all temperatures except for the highest ones (Fig. 8c, left panel).

In order to compare the temperature dependences of the OSSA- and Jaeglé-SSSF and considering that Jaeglé-SSSF does not have a dependency on the wind history, averaged constant values for C_d and H_s were used in the flux calculations applied for the comparison. Although different in origin (through the viscosity in the OSSA-SSSF and through the adjustment to the in-situ measurements in the Jaeglé-SSSF), the variations of the SSSF with SST are similar in the sense that for both SSSFs the production increases with SST and the values for the lowest and highest temperatures are similar (Fig. S3, Supplement). However, the shapes of the relationships are somewhat different. Where the OSSA-SSSF increases monotonously with SST, the Jaeglé-SSSF is much lower in the mid-temperature regime, but rapidly increases at higher temperatures. At this stage, it is difficult to say which dependency is more appropriate as the OSSA-SST dependency derives from first principles, while Jaeglé's comes from the adjustment to in-situ measurements, although, the huge scatter in the data points used in the Jaeglé et al. (2011) study (their Fig. 6) made it difficult to define a precise relationship.

ACPD
13, 23139–23171, 2013

5 Discussion

Introducing the Reynolds number into the OSSA source function brought about improvements as regards the ambiguity in the effect of wind speed and the sensitivity to other environmental parameters. First of all, the scatter at a given wind speed arising from wind history (fetch, rising or waning winds) was reduced by including the wave state into the forcing parameter. Secondly, the Reynolds number encapsulated the SST effects through the viscosity of sea water which depends on its temperature and salinity. Several studies have shown the impact of water temperature on the SSSF (Mårtensson et al., 2003; Sellegri et al., 2006; Jaeglé et al., 2011; Zábori et al., 2012), however, the results from the laboratory experiments were somewhat contradictory or at least not consistent. Mårtensson et al. (2003) showed a decrease in particle number concentration with increasing temperature for particles smaller than 0.35 µm, but an increase for larger particles, while Sellegri et al. (2006) indicated a different threshold at ∼ 0.07 µm; therefore, particles with a diameter of ∼ 0.1 µm would decrease in number concentration for one SSSF, but increase for another one. At the same time, the recent study of Zábori et al. (2012) showed a decrease in number concentration for all particles smaller than 2.5 µm with increasing temperature. In contrast, ambient mass measurement studies (Jaeglé et al., 2011, and references therein) indicated an increase in particle mass with increasing temperature. This mass – temperature dependency is similar to the temperature dependency captured in the OSSA-SSSF, where water temperature effects are included through the kinematic viscosity. The latter was easy to implement into the SSSF and derives from first physical principles, because the terminal velocity of a rising bubble is inversely proportional to the kinematic viscosity of the surrounding fluid. Thus bubbles in warmer waters will rise more quickly to the surface than in colder waters (Lewis and Schwartz, 2004), which would increase the number of smaller bubbles reaching the surface, and thus increase the production of SSA particles (Jaeglé et al., 2011). Also Anguelova and Webster (2006) indicate that

ACPD
13, 23139–23171, 2013

there is an effect of temperature on viscosity, resulting in higher whitecap coverage for warmer waters.

By deriving different flux–Re_{H_w} relationships for different particle size regions, this study accounted for the different effects of wind speed and its history on the shape of the SSSF because each mode has a different dependence on the Reynolds number, thus resulting in different size distributions at different wind speeds or values of the Reynolds number.

Another important advantage of the OSSA source function is that it was derived from in situ observations, from Mace Head and SEASAW; therefore, it lacks many problems which parameterizations based on laboratory experiments are facing, e.g. representativeness of small scale laboratory experiments for oceanic conditions. At the same time coastal stations possess the risk of the effects of the surf zone when SSA fluxes are measured directly. In this study, the SSA fluxes were derived from concentration measurements which are not affected by the coastal effects (Ceburnis et al., 2008). In addition, the specific topography of Mace Head minimises the influence of the surf zone as well (Rinaldi et al., 2009). Moreover, the fact that the two independent and methodologically different datasets used in this study (Mace Head and SEASAW) were so similar in the overlapping size range provided us further confidence in the results.

The present SSSF does not include organic matter which is a very important part of the sea spray aerosol, in particular for the smallest particles (Facchini et al., 2008), which can act as cloud condensation nuclei. Therefore, we suggest to use the OSSA source function to obtain the total sea spray fluxes and to derive the organic fraction by using the parameterisation developed by Rinaldi et al. (2013) in a way it was used before in several other studies (O'Dowd et al., 2008; Vignati et al., 2010; Gantt et al., 2011). There is also evidence that micro-organisms affect the viscosity of sea water (Seuront et al., 2010) so that biological activity may be taken into account via the viscosity, like the effect of temperature and salinity; however, further studies and parameterizations are required on this topic in order to separate the different effects and relate the viscosity to observables like chlorophyll *a* concentrations.

ACPD
13, 23139–23171, 2013

6 Conclusions

The sea spray source function derived in this study covers particle sizes with dry diameters between 15 nm up to 6 µm and encapsulates wave history, salinity and temperature effects through using the Reynolds number as forcing parameter instead of the wind speed. For the first time, this source function shows and accounts for the distinct forcing effects on the different particle size ranges, resulting in different flux distributions for a particular Re_{H_w}. The resulting SSSF provides fluxes which are on the lower side of those calculated using many other source functions developed in the last decade. However, its use results in particle number and mass concentrations closer to the ones measured in real ambient conditions. Better agreement with the measurements allows producing more accurate particle number concentrations and size distributions, which in turn results in a better description of cloud condensation nucleus distribution. The latter is very important in order to reduce the uncertainty in modelling indirect effects on the earth radiative balance arising from primary production of SSA. In addition to climate effects, a correct PM mass assignment to the natural sources, in this case primary marine sea spray aerosol production, is very important in respect to the air quality and source apportionment studies.

Supplementary material related to this article is available online at http://www.atmos-chem-phys-discuss.net/13/23139/2013/acpd-13-23139-2013-supplement.pdf.

Acknowledgements. This work was supported by the European Space Agency (Support To Science Element: Oceanflux Sea Spray Aerosol, contract No. 400 010 4514/11/I-AM), HEA-PRTLI4 Environment and Climate: Impact and Responses programme, and the European Commission 6th Framework programme project EUCAARI (036 833–2), EC ACTRIS Research Infrastructure Action under the 7th Framework Programme, EPA-Ireland, CRAICC (Cryosphere–atmosphere interactions in a changing Arctic climate), part of the Top-level Research Initia-

ACPD
13, 23139–23171, 2013

tive (TRI) of the joint Nordic research and innovation initiative. We would also like to thank Ian Brooks and Sarah Norris, University of Leeds, for making available the SEASAW data and the many discussions on the use of the data, Ernie R. Lewis (Brookhaven National Laboratory) for producing the SSSF intercomparison Figure, Adrian Callaghan (Scripps Institution of Oceanography, UCSD) for the valuable comments and discussions.

References

Abdalla, S., Janssen, P. A. E. M., and Bidlot, J. R.: Jason-2 OGDR wind and wave products: monitoring, validation and assimilation, Mar. Geod., 33, 239–255, doi:10.1080/01490419.2010.487798 239–255, 2010.

Allan, J. D., Jimenez, J. L., Williams, P. I., Alfarra, M. R., Bower, K. N., Jayne, J. T., Coe, H., and Worsnop, D. R.: Quantitative sampling using an Aerodyne aerosol mass spectrometer – 1. Techniques of data interpretation and error analysis, J. Geophys. Res.-Atmos., 108, 4090, doi:10.1029/2002jd002358, 2003.

Anguelova, M. D. and Webster, F.: Whitecap coverage from satellite measurements: a first step toward modeling the variability of oceanic whitecaps, J. Geophys. Res.-Oceans, 111, C03017, doi:10.1029/2005jc003158, 2006.

Blanchard, D. C.: The electrification of the atmosphere by particles from bubbles in the sea, Prog. Oceanogr., 1, 73–202, doi:10.1016/0079-6611(63)90004-1, 1963.

Blanchard, D. C.: Citation-Classic – the electrification of the atmosphere by particles from bubbles in the sea, CC/Phys. Chem. Earth, 48, 16–16, 1986.

Callaghan, A., de Leeuw, G., Cohen, L., and O'Dowd, C. D.: Relationship of oceanic whitecap coverage to wind speed and wind history, Geophys. Res. Lett., 35, L23609, doi:10.1029/2008gl036165, 2008.

Ceburnis, D., O'Dowd, C. D., Jennings, G. S., Facchini, M. C., Emblico, L., Decesari, S., Fuzzi, S., and Sakalys, J.: Marine aerosol chemistry gradients: elucidating primary and secondary processes and fluxes, Geophys. Res. Lett., 35, L07804, doi:10.1029/2008gl033462, 2008.

Clarke, A. D., Owens, S. R., and Zhou, J. C.: An ultrafine sea-salt flux from breaking waves: implications for cloud condensation nuclei in the remote marine atmosphere, J. Geophys. Res.-Atmos., 111, D06202, doi:10.1029/2005jd006565, 2006.

ACPD
13, 23139–23171, 2013

de Leeuw, G., Neele, F. P., Hill, M., Smith, M. H., and Vignali, E.: Production of sea spray aerosol in the surf zone, J. Geophys. Res.-Atmos., 105, 29397–29409, 2000.
de Leeuw, G., Andreas, E. L., Anguelova, M. D., Fairall, C. W., Lewis, E. R., O'Dowd, C., Schulz, M., and Schwartz, S. E.: Production flux of sea spray aerosol, Rev. Geophys., 49, RG2001, doi:10.1029/2010rg000349, 2011.
DeCarlo, P. F., Kimmel, J. R., Trimborn, A., Northway, M. J., Jayne, J. T., Aiken, A. C., Gonin, M., Fuhrer, K., Horvath, T., Docherty, K. S., Worsnop, D. R., and Jimenez, J. L.: Field-deployable, high-resolution, time-of-flight aerosol mass spectrometer, Anal. Chem., 78, 8281–8289, doi:10.1021/Ac061249n, 2006.
Drennan, W. M., Taylor, P. K., and Yelland, M. J.: Parameterizing the sea surface roughness, J. Phys. Oceanogr., 35, 835–848, doi:10.1175/Jpo2704.1, 2005.
Facchini, M. C., Rinaldi, M., Decesari, S., Carbone, C., Finessi, E., Mircea, M., Fuzzi, S., Ceburnis, D., Flanagan, R., Nilsson, E. D., de Leeuw, G., Martino, M., Woeltjen, J., and O'Dowd, C. D.: Primary submicron marine aerosol dominated by insoluble organic colloids and aggregates, Geophys. Res. Lett., 35, L17814, doi:10.1029/2008gl034210, 2008.
Gantt, B., Meskhidze, N., Facchini, M. C., Rinaldi, M., Ceburnis, D., and O'Dowd, C. D.: Wind speed dependent size-resolved parameterization for the organic mass fraction of sea spray aerosol, Atmos. Chem. Phys., 11, 8777–8790, doi:10.5194/acp-11-8777-2011, 2011.
Geever, M., O'Dowd, C. D., van Ekeren, S., Flanagan, R., Nilsson, E. D., de Leeuw, G., and Rannik, U.: Submicron sea spray fluxes, Geophys. Res. Lett., 32, L15810, doi:10.1029/2005gl023081, 2005.
Goddijn-Murphy, L., Woolf, D. K., and Callaghan, A. H.: Parameterizations and algorithms for oceanic whitecap coverage, J. Phys. Oceanogr., 41, 742–756, doi:10.1175/2010jpo4533.1, 2011.
Gong, S. L.: A parameterization of sea-salt aerosol source function for sub- and super-micron particles, Global Biogeochem. Cy., 17, 1097, doi:10.1029/2003gb002079, 2003.
Haeffelin, M., Angelini, F., Morille, Y., Martucci, G., Frey, S., Gobbi, G. P., Lolli, S., O'Dowd, C. D., Sauvage, L., Xueref-Remy, I., Wastine, B., and Feist, D. G.: Evaluation of mixing-height retrievals from automatic profiling lidars and ceilometers in view of future integrated networks in Europe, Bound.-Lay. Meteorol., 143, 49–75, doi:10.1007/s10546-011-9643-z, 2012.
Hill, M. K., Brooks, B. J., Norris, S. J., Smith, M. H., Brooks, I. M., and De Leeuw, G.: A Compact Lightweight Aerosol Spectrometer Probe (CLASP), J. Atmos. Ocean. Tech., 25, 1996–2006, doi:10.1175/2008jtecha1051.1, 2008.

ACPD
13, 23139–23171, 2013

Hoppel, W. A., Frick, G. M., and Fitzgerald, J. W.: Surface source function for sea-salt aerosol and aerosol dry deposition to the ocean surface, J. Geophys. Res.-Atmos., 107, 4382, doi:10.1029/2001jd002014, 2002.

Jaeglé, L., Quinn, P. K., Bates, T. S., Alexander, B., and Lin, J.-T.: Global distribution of sea salt aerosols: new constraints from in situ and remote sensing observations, Atmos. Chem. Phys., 11, 3137–3157, doi:10.5194/acp-11-3137-2011, 2011.

Jimenez, J. L., Jayne, J. T., Shi, Q., Kolb, C. E., Worsnop, D. R., Yourshaw, I., Seinfeld, J. H., Flagan, R. C., Zhang, X. F., Smith, K. A., Morris, J. W., and Davidovits, P.: Ambient aerosol sampling using the Aerodyne Aerosol Mass Spectrometer, J. Geophys. Res.-Atmos., 108, 8425, doi:10.1029/2001JD001213, 2003.

Keene, W. C., Maring, H., Maben, J. R., Kieber, D. J., Pszenny, A. A. P., Dahl, E. E., Izaguirre, M. A., Davis, A. J., Long, M. S., Zhou, X. L., Smoydzin, L., and Sander, R.: Chemical and physical characteristics of nascent aerosols produced by bursting bubbles at a model air–sea interface, J. Geophys. Res.-Atmos., 112, D21202, doi:10.1029/2007jd008464, 2007.

Kleefeld, C., O'Dowd, C. D., O'Reilly, S., Jennings, S. G., Aalto, P., Becker, E., Kunz, G., and de Leeuw, G.: Relative contribution of submicron and supermicron particles to aerosol light scattering in the marine boundary layer, J. Geophys. Res.-Atmos., 107, 8103, doi:10.1029/2000jd000262, 2002.

Lewis, E. R. and Schwartz, S. E.: Sea Salt Aerosol Production: Mechanisms, Methods, Measurements and Models, Geophys. Monogr. Ser., AGU, Washington, DC, 413 pp., 2004.

Mårtensson, E. M., Nilsson, E. D., de Leeuw, G., Cohen, L. H., and Hansson, H. C.: Laboratory simulations and parameterization of the primary marine aerosol production, J. Geophys. Res.-Atmos., 108, 4297, doi:10.1029/2002jd002263, 2003.

Middlebrook, A. M., Bahreini, R., Jimenez, J. L., and Canagaratna, M. R.: Evaluation of composition-dependent collection efficiencies for the aerodyne aerosol mass spectrometer using field data, Aerosol Sci. Tech., 46, 258–271, doi:10.1080/02786826.2011.620041, 2012.

Milroy, C., Martucci, G., Lolli, S., Loaec, S., Sauvage, L., Xueref -Remy, I., Lavric, J. V., Ciais, P., and O'Dowd, C. D.: An assessment of pseudo-operational ground-based light detection and ranging sensors to determine the boundary-layer structure in the coastal atmosphere, Adv. Meteorol., 2012, 929080, doi:10.1155/2012/929080, 2012.

Monahan, E. C. and Muircheartaigh, I. O.: Optimal power-law description of oceanic whitecap coverage dependence on wind-speed, J. Phys. Oceanogr., 10, 2094–2099, 1980.

ACPD
13, 23139–23171, 2013

A sea spray aerosol flux parameterization encapsulating wave state

J. Ovadnevaite et al.

Mulcahy, J. P., O'Dowd, C. D., Jennings, S. G., and Ceburnis, D.: Significant enhancement of aerosol optical depth in marine air under high wind conditions, Geophys. Res. Lett., 35, L16810, doi:10.1029/2008gl034303, 2008.

Nilsson, E. D., Rannik, U., Swietlicki, E., Leck, C., Aalto, P. P., Zhou, J., and Norman, M.: Turbulent aerosol fluxes over the Arctic Ocean – 2. Wind-driven sources from the sea, J. Geophys. Res.-Atmos., 106, 32139–32154, 2001.

Norris, S. J., Brooks, I. M., de Leeuw, G., Smith, M. H., Moerman, M., and Lingard, J. J. N.: Eddy covariance measurements of sea spray particles over the Atlantic Ocean, Atmos. Chem. Phys., 8, 555–563, doi:10.5194/acp-8-555-2008, 2008.

Norris, S. J., Brooks, I. M., Hill, M. K., Brooks, B. J., Smith, M. H., and Sproson, D. A. J.: Eddy covariance measurements of the sea spray aerosol flux over the open ocean, J. Geophys. Res.-Atmos., 117, D07210, doi:10.1029/2011jd016549, 2012.

O'Connor, T. C., Jennings, S. G., and O'Dowd, C. D.: Highlights of fifty years of atmospheric aerosol research at Mace Head, Atmos. Res., 90, 338–355, doi:10.1016/j.atmosres.2008.08.014, 2008.

O'Dowd, C. D., Lowe, J. A., Smith, M. H., and Kaye, A. D.: The relative importance of non-sea-salt sulphate and sea-salt aerosol to the marine cloud condensation nuclei population: an improved multi-component aerosol-cloud droplet parametrization, Q. J. Roy. Meteor. Soc., 125, 1295–1313, 1999.

O'Dowd, C. D., Langmann, B., Varghese, S., Scannell, C., Ceburnis, D., and Facchini, M. C.: A combined organic-inorganic sea-spray source function, Geophys. Res. Lett., 35, L01801, doi:10.1029/2007gl030331, 2008.

O'Dowd, C., Ceburnis, D., Ovadnevaite, J., Rinaldi, M., and Facchini, M. C.: Do anthropogenic or coastal aerosol sources impact on a clean marine aerosol signature at Mace Head?, Atmos. Chem. Phys. Discuss., 13, 7311–7347, doi:10.5194/acpd-13-7311-2013, 2013.

Ovadnevaite, J., Ceburnis, D., Canagaratna, M., Berresheim, H., Bialek, J., Martucci, G., Worsnop, D. R., and O'Dowd, C.: On the effect of wind speed on submicron sea salt mass concentrations and source fluxes, J. Geophys. Res.-Atmos., 117, D16201, doi:10.1029/2011jd017379, 2012.

Petelski, T. and Piskozub, J.: Vertical coarse aerosol fluxes in the atmospheric surface layer over the north polar waters of the Atlantic, J. Geophys. Res.-Oceans, 111, C06039, doi:10.1029/2005jc003295, 2006.

ACPD
13, 23139–23171, 2013

Reid, J. S., Jonsson, H. H., Smith, M. H., and Smirnov, A.: Evolution of the vertical profile and flux of large sea-salt particles in a coastal zone, J. Geophys. Res.-Atmos., 106, 12039–12053, doi:10.1029/2000jd900848, 2001.

Rinaldi, M., Facchini, M. C., Decesari, S., Carbone, C., Finessi, E., Mircea, M., Fuzzi, S., Ceburnis, D., Ehn, M., Kulmala, M., de Leeuw, G., and O'Dowd, C. D.: On the representativeness of coastal aerosol studies to open ocean studies: Mace Head – a case study, Atmos. Chem. Phys., 9, 9635–9646, doi:10.5194/acp-9-9635-2009, 2009.

Rinaldi, M., Fuzzi, S., Decesari, S., Marullo, S., Santoleri, R., Provenzale, A., von Hardenberg, J., Ceburnis, D., Vaishya, A., O'Dowd, C. D., and Facchini, M. C.: Is chlorophyll *a* the best surrogate for organic matter enrichment in submicron primary marine aerosol?, J. Geophys. Res.-Atmos., 118, 4964–4973, doi:10.1002/jgrd.50417, 2013.

Sellegri, K., O'Dowd, C. D., Yoon, Y. J., Jennings, S. G., and de Leeuw, G.: Surfactants and submicron sea spray generation, J. Geophys. Res.-Atmos., 111, D22215, doi:10.1029/2005jd006658, 2006.

Seuront, L., Leterme, S. C., Seymour, J. R., Mitchell, J. G., Ashcroft, D., Noble, W., Thomson, P. G., Davidson, A. T., van den Enden, R., Scott, F. J., Wright, S. W., Schapira, M., Chapperon, C., and Cribb, N.: Role of microbial and phytoplanktonic communities in the control of seawater viscosity off East Antarctica (30–80° E), Deep-Sea Res. Pt. II, 57, 877–886, doi:10.1016/j.dsr2.2008.09.018, 2010.

Sharqawy, M. H., Lienhard V, J. H., and Zubair, S. M.: Thermophysical properties of sea water: a review of existing correlations and data, Desalinization and Water Treatment, 16, 354–380, doi:10.5004/dwt.2010.1079, 2010.

Smith, M. H., Park, P. M., and Consterdine, I. E.: Marine aerosol concentrations and estimated fluxes over the sea, Q. J. Roy. Meteor. Soc., 119, 809–824, doi:10.1256/Smsqj.51210, 1993.

Taylor, J. R.: An Introduction to Error Analysis: The Study of Uncertainties in Physical Measurements, 2nd ed., University Science books, Sausalito, CA, 1997.

Thorpe, S. A.: Bubble clouds and the dynamics of the upper ocean, Q. J. Roy. Meteor. Soc., 118, 1–22, doi:10.1002/qj.49711850302, 1992.

Tsyro, S., Aas, W., Soares, J., Sofiev, M., Berge, H., and Spindler, G.: Modelling of sea salt concentrations over Europe: key uncertainties and comparison with observations, Atmos. Chem. Phys., 11, 10367–10388, doi:10.5194/acp-11-10367-2011, 2011.

ACPD
13, 23139–23171, 2013

Tyree, C. A., Hellion, V. M., Alexandrova, O. A., and Allen, J. O.: Foam droplets generated from natural and artificial seawaters, J. Geophys. Res.-Atmos., 112, D12204, doi:10.1029/2006jd007729, 2007.

Vignati, E., Facchini, M. C., Rinaldi, M., Scannell, C., Ceburnis, D., Sciare, J., Kanakidou, M., Myriokefalitakis, S., Dentener, F., and O'Dowd, C. D.: Global scale emission and distribution of sea-spray aerosol: sea-salt and organic enrichment, Atmos. Environ., 44, 670–677, doi:10.1016/j.atmosenv.2009.11.013, 2010.

Wiedensohler, A., Birmili, W., Nowak, A., Sonntag, A., Weinhold, K., Merkel, M., Wehner, B., Tuch, T., Pfeifer, S., Fiebig, M., Fjäraa, A. M., Asmi, E., Sellegri, K., Depuy, R., Venzac, H., Villani, P., Laj, P., Aalto, P., Ogren, J. A., Swietlicki, E., Williams, P., Roldin, P., Quincey, P., Hüglin, C., Fierz-Schmidhauser, R., Gysel, M., Weingartner, E., Riccobono, F., Santos, S., Grüning, C., Faloon, K., Beddows, D., Harrison, R., Monahan, C., Jennings, S. G., O'Dowd, C. D., Marinoni, A., Horn, H.-G., Keck, L., Jiang, J., Scheckman, J., McMurry, P. H., Deng, Z., Zhao, C. S., Moerman, M., Henzing, B., de Leeuw, G., Löschau, G., and Bastian, S.: Mobility particle size spectrometers: harmonization of technical standards and data structure to facilitate high quality long-term observations of atmospheric particle number size distributions, Atmos. Meas. Tech., 5, 657–685, doi:10.5194/amt-5-657-2012, 2012.

Woolf, D. K.: Parametrization of gas transfer velocities and sea-state-dependent wave breaking, Tellus B, 57, 87–94, doi:10.1111/j.1600-0889.2005.00139.x, 2005.

Wu, J.: Oceanic whitecaps and sea state, J. Phys. Oceanogr., 9, 1064–1068, doi:10.1175/1520-0485(1979)009<1064:Owass>2.0.Co;2, 1979.

Zábori, J., Matisāns, M., Krejci, R., Nilsson, E. D., and Ström, J.: Artificial primary marine aerosol production: a laboratory study with varying water temperature, salinity, and succinic acid concentration, Atmos. Chem. Phys., 12, 10709–10724, doi:10.5194/acp-12-10709-2012, 2012.

Zhao, D. and Toba, Y.: Dependence of whitecap coverage on wind and wind-wave properties, J. Oceanogr., 57, 603–616, doi:10.1023/A:1021215904955, 2001.

ACPD
13, 23139–23171, 2013

Table 1. Lognormal parameters for the SSSF parameterization.

i	σ_i	CMD_i	$\mathrm{F}_i(Re_{H_w})$
1	1.37	0.02	$4.58 \cdot (Re_{H_w}\text{-}1e^5)^{0.556}$
2	1.5	0.048	$0.0045 \cdot (Re_{H_w}\text{-}1e^5)^{1.08}$
3	1.42	0.102	$33.05 \cdot (Re_{H_w}\text{-}1e^5)^{0.545}$
4	1.53	0.279	$1.3 \cdot (Re_{H_w}\text{-}1e^5)^{0.79}$
5	1.85	1.035	$1.02 \cdot (Re_{H_w}\text{-}2e^5)^{0.87}$

ACPD
13, 23139–23171, 2013

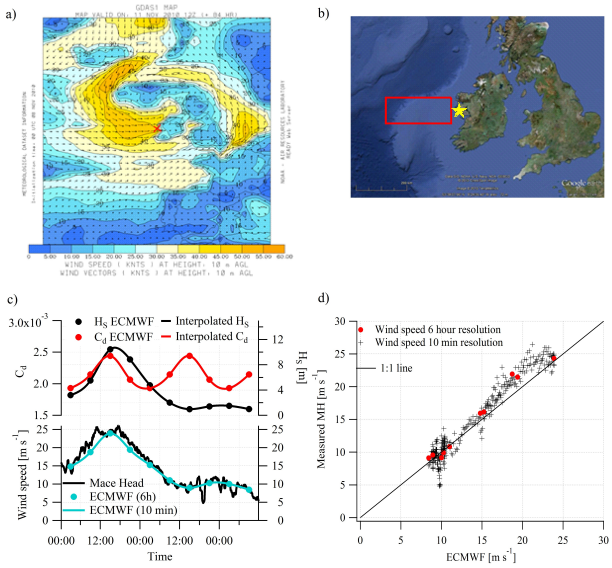

Fig. 1. (a) Wind speed field (in knots) for 12:00 UTC 11 November 2010 obtained from the NOAA Air Resources Laboratory. The local wind speed of 24.1 m s^{-1} (46.8 knots) measured at Mace Head (red cross) was in the range of upwind wind speed presented by NOAA (45–50 knots); **(b)** map of Mace Head location (a yellow star); the red rectangle indicates the area over which the ECMWF parameters were averaged; **(c)** Time series of wind speed measured at Mace Head (MH) and wind speed and wave parameters modelled by ECMWF: H_s – significant height of wind waves, C_d – drag coefficient due to wind waves used for Re_{H_w} calculations; markers represent original 6 hly ECMWF resolution, lines represent the interpolated data to obtain the higher time resolution used for the parameterization. **(d)** Wind speed measured at Mace Head vs. ECMWF modelled wind speed over the area upwind to Mace Head (red area in **(b)**. Red circles represent the original ECMWF resolution and averaged Mace Head measurement, black crosses –10 min measurement averages vs. interpolated ECMWF data.

ACPD
13, 23139–23171, 2013

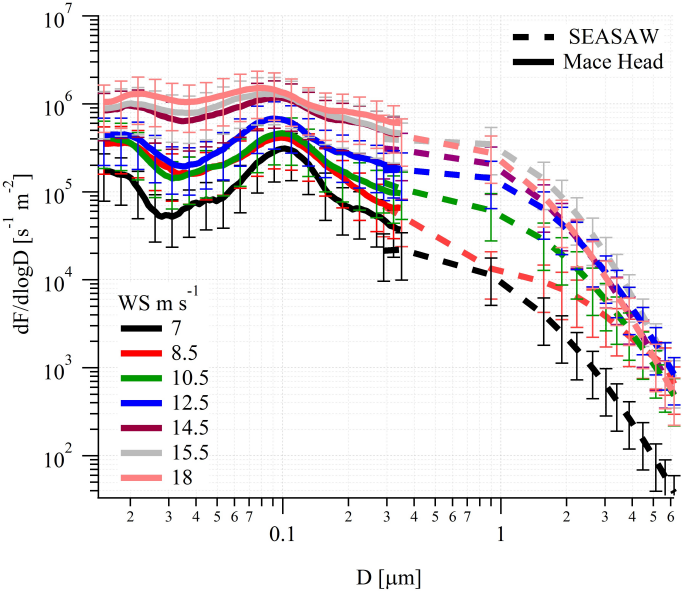

Fig. 2. dF/dlogD at different wind speeds: solid line represents the Mace Head data and dashed line represents SEASAW measurements, error bars represent measurement and method uncertainties described in the Sect. 3.3.

ACPD
13, 23139–23171, 2013

A sea spray aerosol flux parameterization encapsulating wave state

J. Ovadnevaite et al.

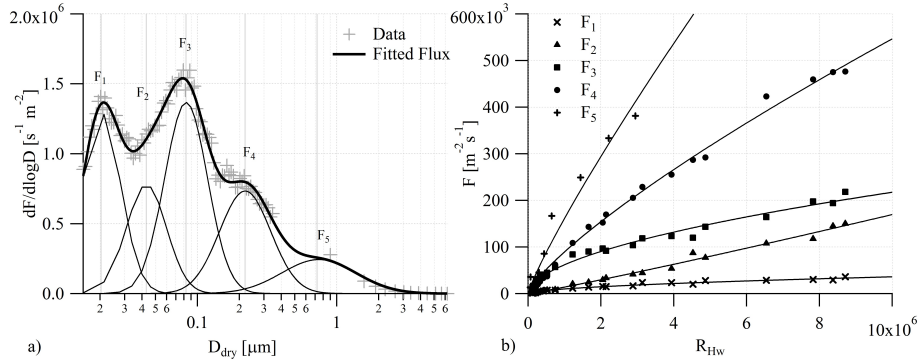

Fig. 3. (a) Parameterization of the size-dependent sea spray aerosol flux at $Re_{H_w} = 3.1\ e^6 (U_{10} \sim 18\,m\,s^{-1})$: markers represent the measured data points, the solid black line represents the parameterization and thin lines represent individual lognormal modes; **(b)** SSA flux vs. Re_{H_w} for the different size modes. Markers represent the measured data points, lines are the fitted power laws used in the parameterization (mode amplitudes F_i, Table 1).

ACPD
13, 23139–23171, 2013

A sea spray aerosol flux parameterization encapsulating wave state

J. Ovadnevaite et al.

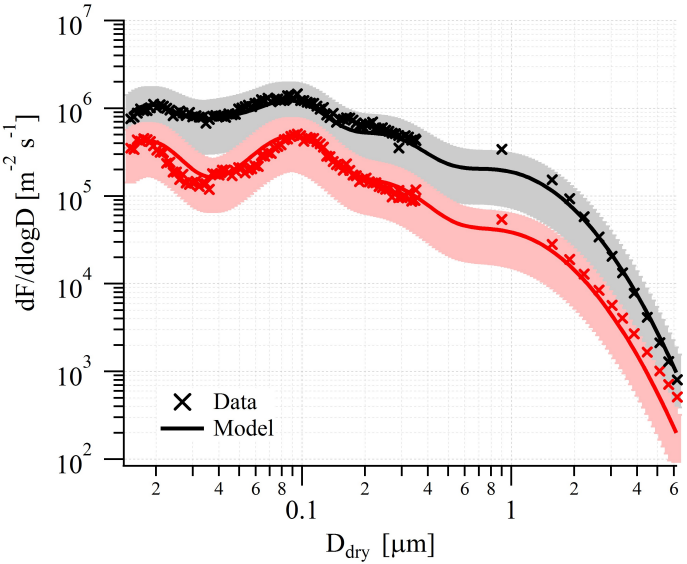

Fig. 4. Size dependent SSSF at two different Re_{H_w}, red at 5.2e^5 ($\sim$ 10 m s^{-1}) and black at 2.2e^6 ($\sim$ 15 m s^{-1}). Markers represent the real data measured at certain wind speed; lines represent calculations from the OSSA source function. Shaded areas represent the SSSF uncertainties.

ACPD
13, 23139–23171, 2013

A sea spray aerosol flux parameterization encapsulating wave state

J. Ovadnevaite et al.

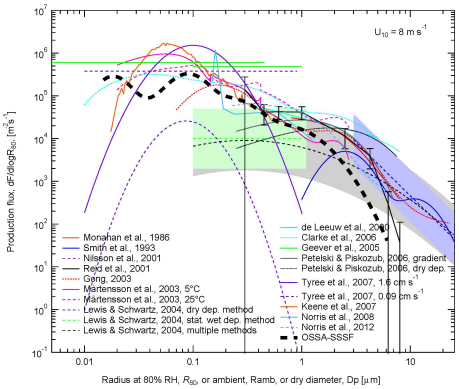

Fig. 5. Comparison of the sea spray source function derived in this study (OSSA-SSSF) with other existing SSSF (Monahan et al., 1986; Smith et al., 1993; de Leeuw et al., 2000; Nilsson et al., 2001; Reid et al., 2001; Gong, 2003; Mårtensson et al., 2003; Lewis and Schwartz, 2004; Geever et al., 2005; Clarke et al., 2006; Petelski and Piskozub, 2006; Keene et al., 2007; Tyree et al., 2007; Norris et al., 2008; Norris et al., 2012), evaluated for wind speed $U_{10} = 8\,\mathrm{m\,s^{-1}}$ (or $U_{22} = 8\,\mathrm{m\,s^{-1}}$ for Geever et al. (2005). Also shown are central values (curves) and associated uncertainty ranges (bands) from review of Lewis and Schwartz (2004), which denote subjective estimates by those investigators based on the statistical wet deposition method (green), the steady state deposition method (blue), and taking into account all available methods (gray); no estimate was provided for $Re_{80} < 0.1$ μm. Lower axis denotes radius at 80 % relative humidity, Re_{80}, except for formulations of Nilsson et al. (2001), Mårtensson et al. (2003), and Clarke et al. (2006) which are in terms of dry particle diameter, D_p, approximately equal to Re_{80} and those of Geever et al. (2005), Petelski and Piskozub (2006) (dry deposition method), and Norris et al. (2008), which are in terms of ambient radius, Re_{amb}. Formulations of Tyree et al. (2007) are for artificial seawater of salinity 33 at the two specified bubble volume fluxes. Formulations of Nilsson et al. (2001) and Geever et al. (2005) of particle number production flux without size resolution are plotted arbitrarily as if the flux is independent of Re_{amb} over the size ranges indicated to yield the measured number flux as an integral over that range. (Figure and caption modified from de Leeuw et al., 2011).

ACPD
13, 23139–23171, 2013

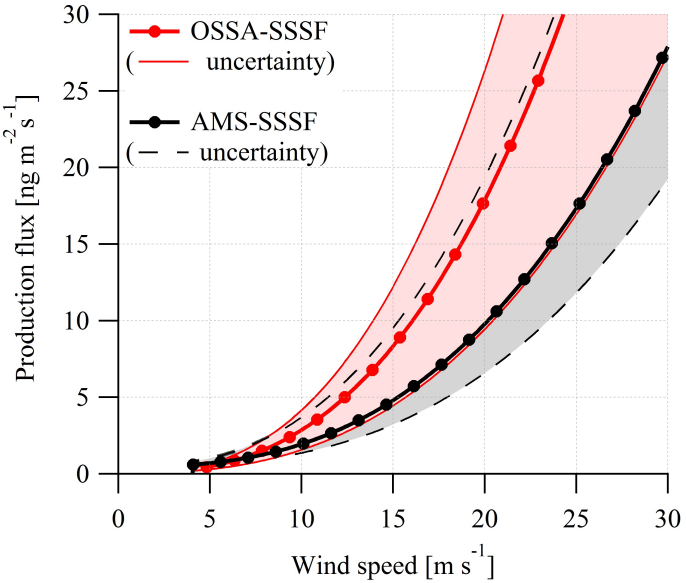

Fig. 6. Comparison between the SSA mass flux calculated using the OSSA-SSSF (see text) (red lines) with the AMS derived mass flux (Ovadnevaite et al., 2012) (black lines) as function of wind speed. Pink and grey areas represent the measurement uncertainties accordingly.

ACPD
13, 23139–23171, 2013

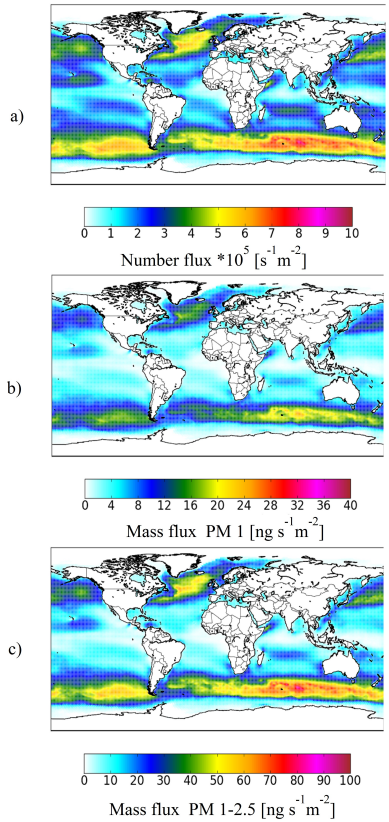

Fig. 7. Annual mean production flux computed using the OSSA-SSSF together with ECMWF meteorological and wave information: **(a)** Number flux of particles smaller than 1 µm; **(b)** Mass flux of particles smaller than 1 µm; **(c)** Mass flux of particles between 1–2.5 µm.

ACPD
13, 23139–23171, 2013

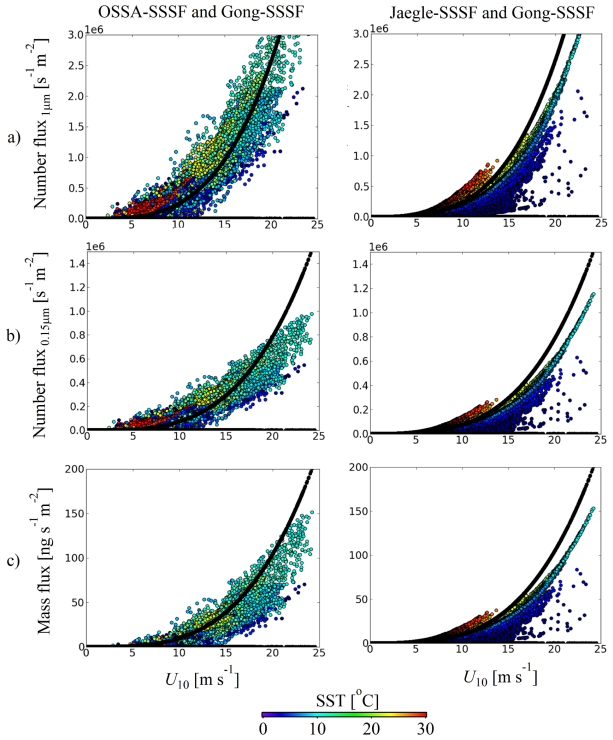

Fig. 8. Global instantaneous (2 Jan 2006, 00:00 UTC) SSA number and mass fluxes; left panel: computed using the OSSA-SSSF (colour circles) overlapped with black dots representing fluxes computed using the Gong (2003) SSSF; right panel: computed using the Jaeglé et al. (2011) SSSF (colour circles) overlapped with black dots representing fluxes computed using the Gong (2003) SSSF; colours represent SST; **(a)** number flux for particles $0.07 < D < 1\,\mu m$; **(b)** number flux for particles $0.07 < D < 0.15\,\mu m$; **(c)** mass flux for particles $0.07 < D < 1\,\mu m$.

ACPD
13, 23139–23171, 2013

A sea spray aerosol flux parameterization encapsulating wave state

J. Ovadnevaite et al.